HHS Public Access

Author manuscript

Dev Biol. Author manuscript; available in PMC 2016 September 01.

Published in final edited form as:

Dev Biol. 2015 September 1; 405(1): 108–122. doi:10.1016/j.ydbio.2015.07.001.

The role of folate metabolism in orofacial development and clefting

Stacey E. Wahl, **Allyson E. Kennedy**, **Brent H. Wyatt**, **Alexander D. Moore**, **Deborah E. Pridgen**, **Amanda M. Cherry**, **Catherine B. Mavila**, and **Amanda J.G. Dickinson***

Virginia Commonwealth University, 1000 West Cary St. Department of Biology, Richmond VA, 23284

Abstract

Folate deficiency has been associated with numerous diseases and birth defects including orofacial defects. However, whether folate has a role in the face during early orofacial development has been unclear. The present study reveals that pharmacological and antisense oligonucleotide mediated inhibition of DHFR, an integral enzyme in the folate pathway, results in specific changes in the size and shape of the midface and embryonic mouth. Such defects are accompanied by a severe reduction in the muscle and cartilage jaw elements without significant change in neural crest pattern or global levels of methylation. We propose that the orofacial defects associated with DHFR deficient function are the result of decreased cell proliferation and increased cell death via DNA damage. In particular, localized apoptosis may also be depleting the cells of the face that express crucial genes for the differentiation of the jaw structures. Folate supplementation is widely known to reduce human risk for orofacial clefts. In the present study, we show that activating folate metabolism can reduce median oral clefts in the primary palate by increasing cell survival. Moreover, we demonstrate that a minor decrease in DHFR function exacerbates median facial clefts caused by RAR inhibition. This work suggests that folate deficiencies could be a major contributing factor to multifactorial orofacial defects.

Graphical abstract

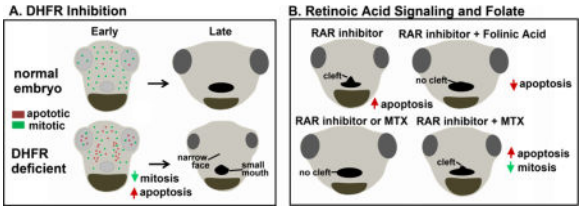

Keywords

Xenopus; Folate; DHFR; orofacial development; retinoic acid and primary palate

*Corresponding author: ajdickinson@vcu.edu.

Introduction

One of the most significant breakthroughs in modern medicine is that mothers can reduce their risk of having a child with a birth defect, such as a neural tube defect or cleft palate, by increasing their intake of folic acid (Wilcox et al., 2007). Why does folic acid have a protective effect for these common birth defects? Moreover, the role of folate metabolism during normal development is not fully understood. Therefore, we began to investigate the role of folate during face formation, with the hope of elucidating a mechanism for the protective properties of folic acid against the development of cleft palate.

Folic acid, folate, or vitamin B9 are terms often used interchangeably to describe a member of the B vitamins that humans need for normal body function (Greenberg et al., 2011). The folate pathway contributes the essential elements necessary for many of the fundamental processes in the cell, such as DNA synthesis and proliferation (reviewed in (Lucock, 2000). Folates are transported into the cell via receptors and transporters, such as reduced folate carriers and folate binding proteins. Inside the cell, folate is converted to dihydrofolate, which is in turn reduced to tetrahydrofolate, by the enzyme dihydrofolate reductase (DHFR). Tetrahydrofolate is a precursor for the synthesis of thymidine and purines, as well as production of S-adenosyl-L-methionine (SAM). Thymidine and purines are essential for DNA/RNA synthesis and repair; therefore, inhibition of folate metabolism could significantly affect growth of the embryo. SAM transfers methyl groups to substrates such as nucleotides, proteins and lipids. A reduction in SAM can thus greatly impact a number of processes, notably epigenetic changes such as DNA and histone methylation, integral to the developing embryo. Certainly, changes in folate metabolism have been shown to affect both DNA synthesis and histone methylation during neurulation, heart development, and in diseases such as cancer (Beaudin and Stover, 2009; Momb et al., 2013; Sun et al., 2011; Tang et al., 2005; Wang et al., 2014). Folate deficiency and mutations to genes involved in the folate pathway cause orofacial defects in model vertebrates and humans (Li et al., 2011; Momb et al., 2013; Tang et al., 2005; Wehby and Murray, 2010; Wilcox et al., 2007) (Burgoon et al., 2002; Kao et al., 2014; Lee et al., 2012). However, it is less clear if these results are due to similar processes during orofacial development.

The orofacial region develops from several facial prominences which grow, converge and differentiate to form the orofacial shape. Such processes are regulated by an intricate network of inductive signals from ectoderm, mesoderm, endoderm and neural crest in each prominence (for review see (Szabo-Rogers et al., 2010)). Formation of the head is therefore a complex orchestra of events that occur in concert. For example, the shape of the orofacial region, including the shape of the embryonic mouth, is intimately tied to the development of the surrounding head (Kennedy and Dickinson, 2014). We therefore asked whether folate metabolism is required for some aspect of this complex developmental event.

In mouse knockouts, it is difficult to separate the effects of gene loss on gastrulation from later development when the mouth and palates form. Additionally, orofacial development is also difficult to track in mouse (due to its in utero development and severe head flexure) and in zebrafish, due to its transparency and small size. Therefore, we have turned to Xenopus to

more easily investigate how folate metabolism modulates orofacial morphogenesis. This is possible because orofacial development is well conserved across vertebrates (Szabo-Rogers et al., 2010). Frog embryos develop ex-utero. In addition, the embryos are large and the face is easily accessible. Moreover, Xenopus embryos are amenable to chemical treatments (Wheeler and Brandli, 2009) and face transplants (Dickinson and Sive, 2009; Jacox et al., 2014b) which allow for temporal and spatial localization of agents that can disrupt folate metabolism. Additionally, we have created a model of primary palate clefting in Xenopus, making this a useful species in which to investigate a role for folate in preventing orofacial clefts.

In the present study we are among the first to show that a deficiency in folate metabolism in the face during early specification of the region results in specific changes in the size and shape of the midface and embryonic mouth. Such defects are accompanied by a severe reduction in the muscle and cartilage jaw elements. We hypothesize that such phenotypic effects of perturbing the folate pathway are the result of decreased cell proliferation and increased cell death. Further, we show that the changes in the folate pathway can affect the formation of retinoic acid receptor (RAR)-induced median clefts of the primary palate. Thus, this study also furthers our understanding of the etiology of multifactorial orofacial clefts.

Methods

Embryos

Xenopus laevis embryos were obtained and cultured using standard methods (Sive et al., 2000). Embryos were staged according to Nieuwkoop and Faber (Nieuwkoop and Faber, 1967).

In situ hybridization

In-situ hybridizations were performed as described (Sive et al., 2000), omitting the proteinase K treatment. DHFR cDNA used to transcribe in-situ hybridization probe was from Open Biosystems and Dharmacon (Clone Id: 6933368, Genbank # BC084841.1). This 812kb sequence was very specific to DHFR and had less that 4% sequence identity with other genes in Xenopus laevis.

DHFR Morpholinos and transplants

Antisense DHFR morpholinos were purchased from Genetools (sequence provided in Supp. Fig. 2). A standard control morpholino provided by Genetools was used as a control. Microinjections were carried out using an Eppendorf microinjector and Zeiss stereoscope. Transplants from morphants to uninjected siblings were performed as described (Dickinson and Sive, 2009).

Chemical treatments

Stock solutions were created of RAR inhibitor (BMS-453, Tocris (3409), 10mM in DMSO), methotrexate (MTX, Sigma, A6770, 100 mM in DMSO) and folinic acid (Sigma, F7878,

100mM in water) and were diluted as described in results section. All chemical treatments were done in 0.1% DMSO in 0.1X MBS and 0.1% DMSO was used as the control.

Immunohistochemistry, phalloidin staining and confocal imaging

Specimens were fixed in 4% PFA and then labeled whole or after vibratome sectioning. For sectioning embryos were embedded in 4% low-melt agarose (SeaPlaque GTG, Cambrex) and sectioned with a 5000 Series Vibratome at 75–100 μm. Immunohistochemistry was performed as described (Dickinson and Sive, 2006) using a rabbit anti-ph3 antibody (Millipore, 06–570, diluted 1:1000) rabbit tri-methyl-histone-H3 (Cell Signaling, 9751S, 1:1000) and rabbit anti-cleaved caspase-3 (Cell Signaling, 9661S, diluted 1:1000). Appropriate secondary AlexaFluor 488 antibodies (Life technologies) were diluted 1:500. Counterstain included 0.1% propidium iodide (Sigma, P4864). Phalloidin labeling was used to visualize muscle (Life Technologies, A12379, diluted 1:50). Images were captured on the Nikon C-1 confocal microscope (VCU, Biology microscopy facility) and assembled using Photoshop (Adobe).

Alcian Blue staining

Cartilages were stained using standard protocols with some modifications (Taylor W, 1985). Briefly, tadpoles were fixed in Bouins fixative overnight at 4°C and then washed in 70% ethanol. They were then immersed in Alcian Blue stain; (0.1mg/ml Alcian Blue in 1 part acetic acid: 4 parts ethanol) for 3–4 days at RT. Embryos were washed in 1% HCL in 70% Ethanol for 1–2 days and cleared in 2% potassium hydroxide and glycerol.

RT-PCR

Total RNA was isolated using Trizol extraction followed by a lithium chloride solution (Ambion, AM9480) precipitation. cDNA was prepared using QuantiTect Reverse Transcription Kit (Qiagen, 205310) and PCR performed. For regular PCR, 2X Hotstart Taq master mix (Apex, 42143) was used with a Bio-Rad thermocycler. For quantitative PCR, SensiFAST SYBR No-Rox (Bioline, BIO-98002) was used with the Bio-Rad CFX96 real time PCR system. The relative amounts of amplification were calculated using delta-delta-CT and were normalized to expression levels of GAPDH. Primer sequences provided upon request.

Protein extraction and Western blot analysis

Western blot analysis was performed as described previously (Dickinson and Sive, 2009). Briefly, embryos were flash frozen in liquid nitrogen and stored or immediately immersed in lysis buffer with protease inhibitors (Sigma Aldrich, S8820). Samples were centrifuged and the protein containing aqueous fraction was obtained by piercing the tube with an 18G needle and extracting said fraction with a syringe. Primary antibodies used were: β-Actin (Cell Signaling, 4970S, 1:1000), β-Actin, (Sigma Aldrich, A5441, 1:5000), histone H3 (Abcam, ab24834, 1:5000), and tri-methyl-histone-H3 (Cell Signaling, 9751S, 1:1000). Secondary antibodies included goat anti-rabbit IgG (Cell Signaling, 5151S) or goat anti-mouse IgG IRDye680 (LICOR, 926–68070) diluted (1:6667). Visualization and quantification was done using the Odyssey CLx Infrared Imaging System and requisite

software (Scanning: Image Studio v.4.0, Quantification: Image Studio Lite v.4.0, LI-COR Biosciences).

Flow cytometry, cell cycle and size analysis

Single cells were isolated using a protocol adapted from (Lee, 2012). Briefly, 25–30 embryos were isolated in 0.5X calcium free Ringer's solution (58 mM NaCl, 1.45 mM KCl, 2.5 mM HEPES pH 7.2) and mechanically digested. After washing, the suspension was chemically digested with 0.25% Trypsin/EDTA (Sigma, T4049) and 5 mg/mL collagenase-II (Worthington, LS004174) for 20 minutes at 37 °C. The suspension was then passed through a 40 μM filter (BD Falcon, 352340), and centrifuged at 4 °C, 3000 rpm for 2 minutes. Cells were resuspended in 5% Goat Serum/PBS and centrifuged again (3000 rpm, 2 minutes, 4 °C). Finally cells were labeled in propidium iodide staining solution (100 mM Tris pH 7.5, 154 mM NaCl, 1 mM CaCl2, 0.5 mM MgCl2, 0.2% BSA, 0.1% Nonidet P-40, 250μg/mL Rnase, 20μg/mL propidium iodide) for 1 hour. FACS analysis was performed using FACSCantoII (BD Biosciences) and the ImageStream flow cytometer (Amnis). Cell shape and size analysis was performed using IDEAS software (Amnis).

Comet Assay

Comet assay was performed as previously described (Dhawan A. et al., 2009). Briefly, tissues from the faces of embryos were immersed in lysis buffer (0.1X MBS with 20 mM EDTA, 10% DMSO) and single cell suspension created with mechanical disruption. Cells were embedded in low melt agarose on a microscope slide and treated with a lysing solution (2.5 M NaCl, 100 mM EDTA, 10 mM Trizma base, 1% Triton X, 10% DMSO, 200mM NAOH, pH=10) for 1–2 hours at 4°C. Slides were placed in a horizontal Bio-Rad gel electrophoresis apparatus with Electrophoresis Buffer (30ml of 10 N NaOH and 5ml of 200 mM EDTA in 1L, pH =13) set at 24 volts for 30 minutes. DNA was labeled with 0.1% propidium iodide and imaged using a confocal microscope.

RESULTS

1. ABROGATED FOLATE METABOLISM CAN REDUCE OR EXACERBATE RETINOIC ACID INHIBITION INDUCED OROFACIAL CLEFTS

Orofacial clefts can be caused by a variety of factors, including vitamin deficiency in the maternal diet. Specifically, adequate retinoic acid (RA) and folate in the maternal diet have been shown to greatly decrease the risk of primary and secondary palate defects. In humans, supplementation with folate or vitamin A (retinoic acid) resulted in reduced cleft lip/palate by 39% and 53% respectively (Boyles, '09). Recently a link between retinoic acid signaling and folate was found in cancer cells (Qi 2006). In acute myelogenous leukemia cells, treatment with all-trans retinoic acid resulted in the upregulation of folate receptor ß (Qi 2006). Our previous work revealed that inhibition of retinoic acid signaling during facial specification in Xenopus results in median clefts in the primary palate (Kennedy and Dickinson, 2012). Due to the known overlap of retinoic acid and folate function during mouth development, we examined the possibility of a link between retinoic acid and folate signaling in orofacial clefting, similar to what was seen in the leukemic cells. The alternative hypothesis is that retinoic acid and folate affect orofacial development through different

mechanisms. If this were the case, utilizing our retinoic acid-inhibition-induced model of orofacial clefts to examine the effects of folate would still provide valuable information about the ability of folic acid to improve orofacial clefting during development. To test both of these possibilities, we performed a treatment with folinic acid, a reduced folic acid analogue, and examined its ability to rescue median clefts induced by retinoic acid inhibition. All embryos were pre-treated with 5 mM of folinic acid for 12 hours. Then, at stage 23/24 (24hpf), embryos were incubated with RAR inhibitor (0.05 μM), fresh folinic acid (5 mM) or RAR inhibitor (0.05 μM) and folinic acid (5 mM) until st. 31/32. Several events occur in the face during this period such as early embryonic mouth development, cranial neural crest migration, and specification of the facial prominences. After treatment, embryos were allowed to develop in normal growth media until st. 42/43, fixed, and analyzed (see schematic Fig. 1A). Embryos treated with DMSO or folinic acid alone looked comparable to untreated controls at stage 42/43 (Fig. 1B,C). Those treated with RAR inhibitor alone had median clefts (100% of embryos examined, Fig. 1D). However, only 16.67% (2/12) embryos treated with folinic acid and RAR inhibitor together appeared to have a malformed mouth shape, while the remainder looked comparable to the controls (Fig. 1E). Facial and embryonic mouth dimensions were measured to further quantify this rescue (Fig. 1F). RAR inhibition resulted in significantly reduced intercanthal distance, reflecting a narrower midface, and an increased face height, reflecting changes in brain position. In addition, these embryos had a smaller mouth angle, and significantly increased midline mouth height. Taken together, these measurements reflected the appearance of a median cleft (Fig. 1G). The folinic acid and RAR inhibitor treated embryos had improved facial measurements that were not statistically different from the controls (Fig. 1G). Overall, these measurements demonstrate that pre-treatment with folinic acid reduces the median cleft phenotype generated by RAR inhibition.

Next, we wondered if the opposite was true, that is, whether decreased folate metabolism exacerbated the median clefts induced by an RAR inhibitor. In these experiments, we used suboptimal concentrations of the RAR inhibitor (0.0125 μM) and a DHFR inhibitor, methotrexate (MTX, 50 μM) over the same stages as described above (stages 24 to 31/32, 22–87hpf). MTX is a synthetic compound that binds DHFR and competitively inhibits folic acid binding (Rajagopalan et al., 2002). The protein sequence and structure of Xenopus DHFR are predicted to be sufficiently conserved for this compound to effectively inhibit DHFR in frogs (see section 3ii and Supp. Fig. 2). After treatment, the embryos were transferred to normal growth media and allowed to develop until st. 42–43 where they were fixed and analyzed (Fig. 1H). At low concentrations of RAR inhibitor or MTX the tadpoles had little or no abnormalities and closely resembled the controls (Fig. 1I–K). In contrast, 97% of embryos treated with a combination of RAR inhibitor and MTX appeared to have a mild median cleft in the primary palate (Fig. 1L). When quantified, the intercanthal distance, mouth height, and mouth angle were significantly different than the control (Fig. 1M). These results suggest that inhibition of folic acid signaling could exacerbate orofacial defects caused by decreased RA signaling.

Together the results from these two experiments sparked multiple questions. For example, does folate interact with retinoic acid signaling? Do these pathways converge on similar processes during development? Such questions were difficult for us to tackle, without a

better understanding the role of folate metabolism during normal orofacial development. Therefore, the remainder of this study focuses on uncovering specific roles of folate metabolism during orofacial development in Xenopus.

2. DHFR IS EXPRESSED IN THE DEVELOPING FACE OF XENOPUS

One of the initial steps in the folate pathway is the reduction of dihydrofolate to tetrahydrofolate by the enzyme dihydrofolate reductase (DHFR). Since DHFR is such a key enzyme in folate metabolism, understanding its role in the developing face could provide important insight into general requirements for folate during orofacial development. Therefore, we first asked when and where DHFR is expressed during early orofacial development. To do this, we performed in-situ hybridization to localize mRNA in the head during early specification and growth of the face (summarized in Supp. Fig. 1). At stages 20–35, DHFR mRNA was observed generally throughout presumptive facial tissues. DHFR mRNA also appeared to be enriched in the eyes and brain during this period. These results suggest DHFR has a role in the developing face and prompted us to further investigate DHFR function during orofacial development.

3. DECREASED FUNCTION OF DHFR USING RESULTED IN FACIAL DEFECTS

To assess the role of DHFR and folate signaling in the development of the face, we used two approaches i) antisense oligonucleotide targeting DHFR and ii) a specific pharmacological inhibitor of DHFR function.

i) Antisense oligonucleotide targeting of DHFR—To examine DHFR function during facial development, we first used a targeted knockdown using antisense oligonucleotides stabilized with morpholino rings (Morpholino (MO), Gene Tools). A sequence that binds to the mRNA at the exon 2-intron 2 boundary and was predicted to result in an exon 2 deletion was synthesized for our analyses (see Supp. Fig. 2). Embryos were injected at the one cell or two-cell stage with 5–7 nl of this splice-blocking DHFR MO (300 μM stock) or an equal amount of standard control MO. By RT-PCR, we observed a smaller transcript and a reduction in the amount of normal spliced DHFR (Supp. Fig. 2C). Control MO injections at the same concentration resulted in 3% abnormal development consistent with uninjected siblings. The abnormalities in DHFR morphants were not apparent until stage 35 (48hpf). These defects were even more pronounced at stage 42–43 (80–87hpf), at which point the tadpoles were examined more closely. DHFR morphants had several developmental defects including a smaller, underdeveloped face (Fig. 2Ai–ii), enlarged pericardial sac or edema in the heart, malformed gut and shorter total body length (Supp Fig. 3A). We quantified general facial size in these DHFR morphants by measuring the intercanthal distance and face height (Fig. 2Aiv). DHFR morphants had a significantly reduced intercanthal distance, while the face height was not different than the controls (Fig. 2Av). Based on the phenotype one might argue that DHFR morphants were simply developing slowly. To address this possibility, we injected DHFR MO into one cell at the 2-cell stage, which localized morpholinos to half of the embryo. These half-DHFR morphants exhibited malformations in the face on the side that was derived from the injected cell (Fig. 2Avi,vii).

To verify the specificity of the DHFR morpholinos we performed rescue experiments with folinic acid. Folinic acid does not require DHFR to be biologically active, thus it can bypass morphant DHFR protein and activate folic acid signaling. Morphants were either incubated with 5mM folinic acid or DMSO soon after they were injected with DHFR morpholinos. Results showed that 95% of the DHFR morphants incubated with folinic acid resembled control embryos (Fig. 2Aviii, ix).

One caveat of our morpholino approach is that the function of DHFR was reduced in the entire embryo. It is therefore difficult to distinguish whether DHFR is specifically required in the face for proper facial development. It is possible that deficient DHFR has an indirect effect on facial development because of its earlier effects on gastrulation, neural tube and/or neural crest specification. To investigate this possibility, we undertook difficult face transplant experiments at stage 23–24 (24hpf) as previously described, to test whether DHFR is required specifically in the face (Dickinson and Sive, 2009; Kennedy and Dickinson, 2012). Control morphant transplants (Fig. 2Bii,ii′) were similar to un-operated controls. DHFR morphant face tissue transplanted to uninjected siblings had malformations consistent with the defects we saw in the face in whole DHFR morphants. Further, increasingly severe facial phenotypes were observed as the size of the morphant tissue increased (Fig. 2Biii–ix′). These results strongly indicate a specific role for DHFR in the tissues of the face.

ii) Pharmacological inhibition of DHFR function—To better define when DHFR is important in orofacial development we next used a pharmacological approach. We bathed embryos in the DHFR inhibitor MTX over early facial development (st. 20–31, 22–37hpf). Similar to DHFR morphants, a phenotype was not apparent until stage 35 (48hpf) and was more obvious at older tadpole stages. Therefore, our phenotypic analyses were performed in stage 42–43 (80–87hpf) tadpoles. We saw an overall increase in the severity of the facial phenotypes with concentrations ranging from 110–440 μM of MTX. This was consistent with concentrations used in zebrafish (Lee et al., 2012) (not shown)). Further, we noted considerable variability in facial phenotypes at each concentration (Supp. Fig. 4). Such inconsistencies in MTX effectiveness have been reported in humans and are thought to be due to a number of factors (Zhao and Goldman, 2003) (and see Supp. Fig. 4 for more discussion). Embryos treated with 220 μM MTX most closely resembled the DHFR morphant phenotype; this dose was used for further analysis. 75% of the faces of embryos treated with 220 μm MTX had a severe or moderate appearance (Fig 3B–E). In these embryos the faces were smaller and underdeveloped similar to what was seen in the DHFR morphants. Upon quantification, we found that the intercanthal distance and the face height were significantly reduced by MTX treatment (Fig. 3F,G).

To verify that MTX treatment affected facial development as a result of inhibiting DHFR, we rescued MTX treated embryos with folinic acid. When embryos were treated with both folinic acid and MTX, the facial dimensions were not statistically different than the controls (Fig. 3D). We also examined the effects of MTX treatment on other embryonic structures and showed decreased embryo length, reduced gut coiling, and heart abnormalities that closely resemble the DHFR morphants (representative images in Supp. Fig. 3B). The

similarity in the phenotype produced by MTX treatment and DHFR morpholino is further evidence of specificity of MTX activity in Xenopus.

Taken together the MTX and DHFR morphant data indicate that DHFR function is specifically required for orofacial development during early specification events in the face. In the next sections we aimed to better characterize the facial phenotypes of embryos deficient in DHFR function. To do this we primarily used MTX treated embryos since we could more easily control the timing of the application and set up numerous experiments with ease.

4. QUANTIFICATION OF FACIAL DIMENSIONS REVEALED SPECIFIC CHANGES IN OROFACIAL SHAPE IN EMBRYOS WITH DECREASED DHFR FUNCTION

One might argue that the reduction of folate metabolism results in such a growth delay, based on casual observations of the smaller size of the embryo. If this were the case, we would expect that the face would be smaller without a change in the shape of facial features. To test this, we performed geometric morphometrics to evaluate changes in face shape (Kennedy and Dickinson, 2014a; Kennedy and Dickinson, 2014b). Briefly, 31 facial landmarks were chosen to best represent the shape of the face (Fig. 3H). MorphoJ analysis software aligned the landmarks using superimposition algorithms to eliminate differences in the size of the embryos. The multivariate statistical technique, canonical variate analysis (CVA), was then applied to landmark data to reveal how the control and MTX treated embryos differed in facial shape (Fig. 3I). We performed this analysis on embryos treated with MTX and folinic acid, our previously described rescue group at st. 42. As indicated by the spread of points on the graph, there is considerable variation among individuals. Despite such variability, the difference between the control and MTX treated embryos was statistically significant (p-value< 0.001). While there was an observable difference between control and our rescue, the groups were more similar to each other than either was to the MTX treated group (Fig. 3I). To visualize how the position of an individual landmark changed between control and MTX-treated embryos, vectors of landmark displacement were superimposed on a transformation grid (Fig. 3J, top grid). The most striking changes in landmark position were those on the lateral edges of the face as well as those around the mouth. Warping of the grid showed shape changes in the midface, which is consistent with the facial narrowing seen in MTX treated embryos (Fig. 3J, top grid). When the same analysis was performed with control and rescue embryos, the largest changes observed were at the periphery of the face. In fact, the mouths of the control and rescue groups were very similar, providing evidence that the folinic acid treatment was indeed rescuing the changes to mouth shape induced by MTX (Fig. 3J, bottom grid).

There is a long time between the MTX treatment, which occurred during early facial specification events and stage 42 when the jaw elements of the face form. Therefore, we also examined the size and shape of the face at stage 40 to determine if similar changes in face dimensions and shape could also be detected. At st. 40 (66 hpf), the intercanthal distance was also reduced in MTX-treated embryos compared to control, while the facial height was not significantly different (n=37, Supp. Fig. 7B). Morphometric analysis of MTX treated

embryos at st. 40 also revealed similar albeit less dramatic changes in facial shape as those at stage 42 (Supp. Fig. 7B, n=37, $p<0.05$).

In summary, our facial analyses show that MTX treated embryos do indeed exhibit differences in facial shape, refuting the simplistic interpretation that folate signaling resulted in a generic developmental delay and thus a smaller embryo. Further, treatment with folinic acid bypasses the inhibition of folate signaling by MTX and partially rescues these facial shape changes.

5. CARTILAGE AND MUSCLE ANATOMY WAS ALTERED IN EMBRYOS WITH DECREASED DHFR FUNCTION

Our data above reveals that DHFR inhibition results in changes in both size and shape of the developing orofacial region. Since the shape of the orofacial region is very much dependant on the formation of structures in the head such as cartilage and muscle (which give the face much of its form during early tadpole stages), we next examined these structures. To examine the effect of deficient DHFR function on the development of these jaw elements, we examined anatomical changes in muscle using a marker for F-actin, phalloidin, and in cartilage using Alcian Blue staining. Embryos were treated MTX as described above (stages 20–31, 22–37hpf). MTX was removed at st. 31 and the tadpoles were allowed to develop until approximately stage 45 (98hpf) when muscle and cartilage in the jaw are well formed (Fig. 4A). Several jaw muscle elements were identified in control embryos such as the hyoid arch, branchial arch, and hypobrachial muscles (Fig. 4B). DHFR inhibition resulted in unrecognizable concentrations of F-actin labeling in the posterior of the head that were not consistent from one embryo to the next (representative images Fig. 4C,D). Cartilage was well formed in the controls where the quadrate, ethmoid, Meckel's, ceratohyal, elements were identifiable (Fig. 4E). In MTX treated tadpoles, there was a noticeable decrease in facial cartilages but like the muscle, this decrease was inconsistent among individual embryos (representative images Fig. 4F,G). The decrease in the jaw muscle and cartilage elements in MTX treated embryos was consistent with the decreased size and malformed shape of the face (see Fig. 3). Further, the variability in facial shape of MTX treated embryos as described by our morphometric analysis correlated with such inconsistent changes in these jaw structures.

6. DHFR INHIBITION RESULTED IN UNCHANGED NEURAL CREST MARKER PATTERN BUT DECREASED LEVELS

The decrease in jaw cartilage and muscle could be attributed to many problems such as differentiation, proliferation, or survival of the tissues that form and influence jaw development. Such tissues include neural crest which itself develops into the jaw cartilage and also induces mesoderm to form the jaw muscle (Noden and Francis-West, 2006) (Grenier et al., 2009; Schmidt et al., 2013; Simoes-Costa and Bronner, 2015). Previous work showed that a folate carrier protein is essential for proper neural crest development in Xenopus and zebrafish (Li et al., 2011; Sun et al., 2007). We therefore tested whether embryos deficient in DHFR function during early facial development had defects in neural crest abundance and/or patterning. To do this, the expression of a neural crest cell marker, AP-2 was examined by RT-PCR and in-situ hybridization respectively (de Croze et al.,

2011; Winning et al., 1991). The pattern of AP-2 mRNA expression in the head and presumptive facial area was similar in the controls and MTX-treated embryos at st. 32–35 (40–50 hpf). As a preliminary quantitative assessment, we measured the AP-2 mRNA expression region, at st. 32–35, to the left of the stomodeum, where a striped expression pattern was observed (Fig. 4Hii, asterisk). This was plotted relative to the height of the face, which we measured as the midline from the top of the cement gland to the top of the eyes. We found no significant difference in the AP-2 expression domain around the embryonic mouth between controls and MTX treated embryos (Fig. 4I). While there didn't seem to be significant change in AP-2 pattern, we did notice that many of the MTX treated embryos were more faintly labeled for AP-2. To address this and provide a more accurate measurement of AP-2 expression levels, we used quantitative RT-PCR. Embryos treated with MTX had indeed slightly but significantly reduced levels of AP-2 relative to controls (Fig. 4J). We next examined expression pattern of AP-2 in MTX-treated embryos at st. 40 (66 hpf) and found that there was a more dramatic loss of the marker around the mouth (Supp. Fig. 7C). These results seem to indicate that there is a gradual reduction in neural crest in the orofacial region after it is specified and has migrated.

7. DHFR INHIBITION REDUCED EXPRESSION OF GENES IMPORTANT FOR CRANIOFACIAL DEVELOPMENT BUT DID NOT ALTER GLOBAL METHYLATION

Since we saw that the levels of a neural crest marker gene were reduced in MTX treated embryos, at st. 32–35 (40–50 hpf), we next sought to investigate the expression of other genes crucial for development of the face when DHFR was inhibited in the same time frame. Changes in such gene expression could explain some of the facial size and shape changes observed in embryos with decreased DHFR function. The mRNA levels relative to GAPDH were generally all decreased, with a statistically significant decrease in fgf8, rarg and wnt8 expression (Fig. 4K). These results suggest the possibility that DHFR function is required for proper gene expression in the face.

It has been well established that folate metabolism provides requirements for many types of methylation reactions. Specifically, previous work in Xenopus has shown that disruption of folate carrier protein affects tri-methylation of H3K4 (Li et al., 2011). Since this methylation mark is essential for active transcription we hypothesized that changes in H3K4me3 could also account for a general decrease in gene expression that we describe above. Therefore, our next goal was to determine if DHFR deficiency results in decreased tri-methylation of H3K4. To do this we took two approaches; i) immunohistochemistry to visualize local effects in the face and ii) western blot approach to quantify changes in H3K4me3 levels relative to total histone H3. In transverse sections of the face, H3K4me3 immunohistochemistry appeared slightly decreased especially in the brain and the eye of MTX-treated embryos (Fig. 4L,M). We further tested the specificity of this result by injecting the morpholino in one cell at the 2-cell stage, resulting in DHFR inhibition in half of the embryo. In these embryos, there again was a slight decrease in H3K4Me3 on the injected side (Supp. Fig. 8A–A″). By western blot, there was a decrease in both tri-methylated and total histone protein in MTX treated embryos (Fig. 4N). However, there was no change in the ratio of methylated to total histone H3 in embryos treated with MTX (Fig.

4O) suggesting that methylation was unchanged but the total levels of the histone H3 were decreased.

We also examined global levels of DNA methylation using a simple methylation sensitive restriction digest approach (see Supp. Fig. 5 for more details). Results from these experiments indicated that there are no dramatic changes in global DNA methylation in embryos treated with MTX compared to controls.

The results from these investigations into the methylation status of MTX-treated embryos show that while DHFR deficiency does cause a general decrease in gene expression, it does not dramatically alter global methylation of histones and DNA during early face development. However, DHFR function may be necessary for maintaining total histone H3 levels. Decreased histone levels can be a consequence of abnormalities in cell division and cell survival (O'Sullivan et al., 2010; Soto et al., 2004; Wu et al., 2002), both of which we explore in the next sections.

8. DHFR INHIBITION RESULTED IN CHANGES IN CELL CYCLE DURING FACIAL DEVELOPMENT

In addition to providing substrates for methylation reactions, folate metabolism provides elements critical for DNA synthesis and is therefore integral for cell division. Further, previous work in zebrafish and mouse have shown that decreased DHFR function or loss of a folate binding proteins cause a decrease in cell cycle progression, particularly through S-phase (Lee et al., 2012; Tang et al., 2005). Therefore, we hypothesized that the changes in face shape and size observed with DHFR inhibition in Xenopus could be due to perturbations in cell cycle progression and subsequent decreases in cellular division. To test this hypothesis we again took two approaches; i) we examined the phosphorylation of histone H3 (ph3) a marker of mitosis (Hans and Dimitrov, 2001) and ii) we used FACS analysis to characterize and quantify changes in cell cycle profiles in embryos treated with MTX (Fig. 5A). MTX treatment resulted in a possible overall decrease in the number of ph3 positive cells in the face compared to controls (Fig. 5Bi–iii, 2 representative images). However, such a decrease was variable and not consistent in any location making it difficult to quantify. When the morpholino was injected in one cell at the 2-cell stage, a slight decrease in ph3 was observed in the injected side (Supp. Fig. 8B–B″), suggesting the decreased observed in MTX-treated embryos was a specific effect. We next utilized propidium iodide labeling and FACS analysis to provide quantifiable data to describe the cell cycle. DHFR inhibition showed a small but significant decrease in the percentage of cells in G2/M compared to control suggesting that there are slightly less mitotic activity in MTX treated embryos, supporting the pH3 data (Fig. 5Ci for representative plots, Fig. 5Cii for averages and Supp. Fig. 6A for data table). Interestingly, MTX treatment also resulted in a significant increase in the percentage of cells in the sub-G1 fraction and a decrease the percentage of cells in the G0/G1 phase. The sub-G1 fraction contains cells that have lost some DNA content, which is most often attributed to cell death (George et al., 2004) (Fig. 5Ci,ii). An increase in sub-G1 and corresponding decrease in G0/G1, which is comprised of cells not undergoing cell division, reflects a possible increase in apoptotic cells in embryos deficient in functional DHFR. We were also interested to see that, contrary to what was

predicted based on studies in zebrafish and mouse; there was no change in the percentage of cells in S-phase. However, it is possible that the time chosen for our analysis resulted in us missing any such changes. Therefore, we additionally performed a cell cycle profile analysis directly after MTX treatments at stage 31–32 (80–87hpf) as well as at stage 40. At stage 31/32 results showed only a significant change in G2/M phase (Supp. Fig. 6). At stage 40 the cell cycle profiles largely mirrored stage 35/37 (Supp. 7D) with the exception that there was a more dramatic increase in the sub-G1 phase suggesting more apoptosis. Further, the protein level of proliferating cell nuclear antigen (PCNA), a specific marker of S-phase, was not different in MTX treated embryos (representative blot, Supp. Fig. 6).

Taken together our cell cycle analysis suggests that DHFR inhibition may affect cell-cycle progression through mitosis, however this may not be due to decreased progression through S-phase. Instead MTX treatment may eventually be causing cells to undergo apoptosis.

9. DHFR INHIBITION INCREASED APOPTOSIS IN THE DEVELOPING FACE

There is considerable evidence to support the idea that decreased folate metabolism can result in increased apoptosis in animal models and cell lines (for some examples see (Tang et al., 2005; Wang et al., 2014; Zhang et al., 2009))(Li et al., 2003). To determine if decreased DHFR function also increased cell death in Xenopus orofacial development we; i) performed immunohistochemistry for cleaved caspase-3 in the face as well as ii) examined and quantified cell morphology by FACS analysis in embryos deficient for DHFR function.

Since caspase-3 is a main effector of the apoptotic process and is activated by its cleavage we asked whether there was a change in cleaved caspase-3 in embryos deficient for DHFR function (Porter and Janicke, 1999). Embryos treated with MTX had a dramatic increase in cleaved caspase-3 positive cells in the orofacial region (Fig. 6Bi–iii). In particular such putative apoptotic cells were localized throughout the face, eyes and brain in a variable pattern. The same result was observed when embryos were injected with the DHFR morpholino at the one or two-cell stage (Fig. 6Biv–vi, Supp. Fig. 7E and 8C–C″, 8D–D″). These results indicate that DHFR inhibition indeed resulted in a specific increase in apoptosis.

During apoptosis the cell shape becomes distorted resulting in an increase in perimeter, without a change in area, and an aspect ratio, minor axis relative to the major axis, that is less than one (George et al., 2004) (Fig. 6Ci). Therefore, we next measured perimeter and aspect ratio of cells as a predictor of apoptosis using the ImageStream flow cytometer. Cells isolated from MTX-treated embryos did indeed have a significant increase in perimeter without changes in area and a significant decrease in the aspect ratio (Fig. 6Cii). Upon closer inspection of individual cells, many appeared abnormally shaped with blebs characteristic of dying cells (representative images Fig. 6Ciii). These results provide further evidence that DHFR inhibition results in increased apoptosis.

Next we wanted to determine what causes the increase in apoptosis in embryos with deficient DHFR function. There are several mechanisms by which apoptosis could be occurring when DHFR is inhibited, including increased oxidative stress and failed DNA repair mechanisms. Since both of these mechanisms could result in DNA damage, we next

examined whether inhibition of DHFR could cause in an increase in damaged DNA in the faces of embryos treated with MTX (Fig. 6A). To do this we used a single cell electrophoresis method called a comet assay, in which damaged or fragmented DNA moves further from the nucleus when exposed to an electrical gradient than undamaged DNA (Fig. 6Di). Thus, cells with damaged DNA generate a comet appearance when labeled with propidium iodide. Propidium iodide fluorescence, reflecting DNA content, was quantified in the "comet tail" in cells derived from the faces of MTX treated and control embryos. DHFR inhibition resulted in a significantly higher amount of DNA in comet tails compared to the controls (Fig. 6Dii–iv). Thus, these results indicated that DHFR inhibition resulted in increased DNA damage, possibly leading to increased apoptosis.

If the decrease in folate metabolism results in accumulated DNA damage leading to apoptosis then we might expect that at later stages of development we might see a more dramatic increase in cell death. At stage 40 we did indeed see a more pronounced portion of cells in the sub-G1 phase as well as more cleaved caspase-3 labeling in the face (Supp. Fig 7D, E). These results also explain the more dramatic effects on facial morphology later in development.

10. FOLINIC ACID SUPPLEMENTATION INCREASED CELL SURVIVAL IN EMBRYOS TREATED WITH AN RAR INHIBITOR

The results presented here reveal that a deficiency in folate metabolism caused a decrease in cell division and an increase in apoptosis in the early developing face. Therefore, we wondered whether folate supplementation could correct for an imbalance in cell proliferation and/or survival in embryos with an orofacial defect. Our previous work also showed that inhibition of RAR results in reduced cell division in the face correlating with a median cleft in the primary palate. We examined the effects of folinic acid on cell division in RAR inhibitor treated embryos. Under the conditions of low levels of RAR inhibitor we could not detect a significant change in proliferation in any group (data not shown). Therefore, we examined whether folinic acid could reduce levels of apoptosis in embryos treated with a higher concentration RAR inhibitor. Embryos were treated with RAR inhibitor and folinic acid together or each chemical alone as described above in section 1. Our results revealed that RAR inhibitor alone resulted in a qualitative increase in apoptotic cells in the midface in all embryos (Fig. 7A,B). Embryos treated with both folinic acid and RAR inhibitor did not appear different than the controls (Fig. 7C).

DISCUSSION

The present study is among the first to focus on a role for folate metabolism exclusively in the face during orofacial development. We show that DHFR deficiency specifically during early head and facial development causes a narrower midface and malformed mouth shape, due to loss of jaw muscle and cartilage elements. This is consistent with reported effects in mammals where folate deficiencies or mutations to major pathway components can also result in craniofacial defects and smaller head size (Burgoon et al., 2002; Momb et al., 2013; Tang et al., 2005; Wang et al., 2014; Zhao et al., 2013). Further, DHFR mutations are associated with cleft lip in humans (Martinelli et al., 2014). Therefore, a conserved role for

folate metabolism in the developing vertebrate face is likely. Importantly, our present study indicates that DHFR is needed for multiple processes such as cell division, gene expression, and cell survival during development of the orofacial region. Most significantly, we demonstrate that folate metabolism can positively influence orofacial clefting in a retinoic-acid inhibition induced model of cleft palate. Stimulating the folate pathway can increase cell survival and prevent median clefts of the primary palate.

1. DHFR is required in the face during early orofacial development

It has been suggested that the facial defects associated with folate deficiency may simply be a consequence of problems with neural tube closure and cranial neural crest specification (Finnell et al., 1998; Finnell et al., 2004). Certainly, mice and Xenopus deficient in folate receptors, folb1 or RFC respectively, have aberrant cranial neural crest development accompanied by later craniofacial defects (Li et al., 2011; Tang et al., 2005). However, we propose that the folate pathway is also critical in the cells of the face during early orofacial development. We tested this hypothesis by examining the role of DHFR in the face after neural tube closure and neural crest specification, something that has not been tested in a vertebrate model to date. Our work shows that DHFR is required in the presumptive face during embryonic mouth and facial prominence specification (Dickinson and Sive, 2009; Jacox et al., 2014a; Kennedy and Dickinson, 2012). Not only is DHFR expressed throughout the face during this time, an inhibitor of DHFR (methotrexate) resulted in a malformed face when administered over this period. Further, DHFR morphant face tissue transplanted to a wild-type embryo with a normal brain and normally specified neural crest still exhibited facial defects. DHFR inhibition over early orofacial development results in a normal neural crest pattern but later neural crest derivatives, such as jaw cartilage, as well as mesoderm derivatives, such as muscle, are severely reduced. Such observations suggest that folate signaling may have more widespread effects in later development of the face. Therefore, our work next focused on defining the processes that are disrupted in the orofacial region when DHFR function is inhibited.

2. What causes the DHFR deficient facial phenotypes?

Why does DHFR inhibition result in specific defects in the shape and size of the midface and mouth? Folate metabolism performs major housekeeping functions in the cell by synthesizing substrates necessary for DNA synthesis and repair as well as methylation of DNA, protein and RNA. Therefore, we might predict that reduction in the function of an essential enzyme at the top of this pathway, such as DHFR, could broadly impact tissue growth, epigenetics and/or cell survival in the embryo.

i) A Reduction in cell proliferation could contribute to DHFR inhibition induced facial abnormalities—We predicted that DHFR inhibition would decrease mitotic rates thereby impacting orofacial growth and morphogenesis. Our results show that there are on average 4% less mitotic cells in Xenopus embryos with deficient DHFR function. While this seems a minor change, our cell cycle analysis represents only a snapshot at one stage in development. Thus, it is likely that this small decrease in mitosis is compounded over time and could result in a significant reduction in growth of the embryo. Such a reduction could at least in part account for the progressively more apparent decrease

in the size of the face during the development of MTX-treated embryos and DHFR morphants. Folate deficiency or mutations to folate pathway genes can also result in low birth weight in humans and a smaller embryonic size in model vertebrates, with specific defects in cell cycle progression in zebrafish (Lee et al., 2012; Molloy et al., 2008; Momb et al., 2013; Sun et al., 2011)Lee, 2012). However, decreased proliferation alone could not account for the facial shape changes and lack of differentiation of the jaw muscle and cartilage.

ii) Global changes in methylation are not a major contributor to the DHFR inhibition induced facial abnormalities—In addition to contributing to nucleotide synthesis, the folate pathway also plays a critical role in the synthesis of S-adenosylmethionine (SAM), which serves as the methyl group donor in DNA, RNA and protein methylation reactions. Since both histone and DNA methylation are important epigenetic regulators we predicted that a lack of DHFR function could result in major changes in gene expression, by altering global methylation levels as has been reported in adult systems (Choi et al., 2005; Ichi et al., 2010; Shookhoff and Gallicano, 2010). While our present study does reveal that DHFR inhibition results in a decrease in gene expression, especially genes important for jaw development such as RARg, fgf8 and wnt8a, we did not observe a correlative change in global levels of tri-methylated H3K4 or DNA methylation. Similarly, gene expression changes were not correlated to changes in DNA methylation in folate depleted human cell lines (Crott et al., 2008). Few studies actually support the prediction that folate deficiency causes large-scale changes in methylation during development so our results were unsurprising (Chang et al., 2011). Also, disrupted neural crest gene expression by reduced folate carrier might be mediated by tri-methylation of H3K4 in Xenopus (Li et al., 2011). Based on these studies we speculate that disrupting folate metabolism early in development, prior to neural crest specification, may have more impact on methylation changes than disruption later during orofacial development. In our work, we also cannot exclude the possibility that DHFR inhibition did induce selective changes in histone or DNA methylation associated with specific genes expressed in the face, and global assays were not sensitive enough to detect this change. Regardless, our experiments do show that large-scale changes in methylation are not a major contributor to DHFR inhibition induced changes in gene expression and orofacial defects.

iii) Apoptosis is a major contributor of DHFR inhibition induced facial abnormalities—Folate metabolism generates a number of essential elements for basic cellular functions; we predicted that cell survival could be compromised in DHFR deficient embryos. Apoptosis is characterized by activation of caspase-3 followed by decreased transcription, nucleosome release and membrane blebbing (Elmore, 2007). We observed these apoptotic features when DHFR function was blocked in Xenopus embryos. This is consistent with reports in other vertebrates where defects in folate metabolism also resulted in increased apoptosis during development (Lee et al., 2012; Sun et al., 2014; Tang et al., 2005; Wang et al., 2014). Moreover, we demonstrated that DHFR inhibition induced apoptosis is in part due to increased DNA damage. This was not a surprise, since cells with defective folate metabolism would fail to generate sufficient thymidine, which can lead to genomic instability and DNA damage (Andersen et al., 2005; Gu et al., 2002; Novakovic et

al., 2006; Zhao et al., 2013). Additionally, oxidative stress generated when the folate pathway is abrogated can cause DNA damage-induced cell death (Bagnyukova et al., 2008; Ho et al., 2003; Kao et al., 2014; Rogers et al., 2007). DNA damage could be a conserved effect of DHFR deficiency since MTX treated tumor cells also have increased DNA damage (Martin et al., 2009) and children with folic acid deficiencies have increased levels of DNA damage in the palate (Brooklyin et al., 2014).

Importantly, our work suggests that apoptosis is the major contributor to the orofacial defects observed in embryos with deficient DHFR function. Cleaved caspase-3 positive cells localized to regions of the face that correlated well with shape changes that were identified in the midface by geometric morphometrics. In addition, developmental genes important for cartilage and muscle differentiation such as RAR receptors, fgfs and wnts are expressed in the midface region, where there are abundant apoptotic cells. Thus, we propose that defects in folic acid metabolism during facial development also results in the depletion of cells expressing genes essential for facial structure formation. Together, loss of gene expression and region specific apoptosis can profoundly affect the shape and size of the face.

3. Multifactorial orofacial clefts, role of folate and retinoic acid

Understanding why some people develop orofacial clefts and others do not is an important human health question. We have previously shown that retinoic acid inhibition results in a median orofacial cleft in Xenopus. Here, we demonstrate that problems in folate metabolism could exacerbate minor deficiencies in endogenous signals during development and thus explain the multifactorial nature of such birth defects. It is possible that folate metabolism is required for retinoic acid signals in the face. Certainly, RARg expression is decreased upon DHFR inhibition. It is also possible that both folate and retinoic acid deficiencies affect similar cellular processes such as apoptosis or mitosis (see below and Fig. 7E). Together these effects can be compounded. Regardless of the mechanism, we propose that defects in folate metabolism during embryonic development could “bring out” a genetic predisposition or worsen an exposure to chemical agent in humans.

Understanding why folic acid supplementation reduces the incidence of cleft palate in humans could help develop additional preventative treatments as well as a better understanding the causes of orofacial clefts. In our experiments, we show that folinic acid supplementation reduced the median clefts induced by RAR inhibition in Xenopus. One mechanism by which such supplementation might prevent median clefts is by enhancing cell survival or boosting proliferation (Fig. 7D). Certainly, our work provides at least evidence of the former. On the other hand, other research has shown that excess folate supplementation is not always beneficial during development and its effectiveness could depend on genetic factors (Marean et al., 2011). Therefore, we believe we have created a useful model for better understanding how gene-environment interactions can influence complex developmental processes.

In conclusion, our work is a first step in understanding how folate supplementation and deficiency can affect orofacial development.

Supplementary Material

Refer to Web version on PubMed Central for supplementary material.

Acknowledgments

This work was supported by NIH grant RDE023553A to Amanda Dickinson. This work was partially supported by the Flow Cytometry Core grant NIH Grant P30CA16059. We would like to thank Greg Walsh, Maria Rivera, Rita Shiang and Rob Tombes for their suggestions concerning the project.

References

Andersen S, Heine T, Sneve R, Konig I, Krokan HE, Epe B, Nilsen H. Incorporation of dUMP into DNA is a major source of spontaneous DNA damage, while excision of uracil is not required for cytotoxicity of fluoropyrimidines in mouse embryonic fibroblasts. Carcinogenesis. 2005; 26:547–55. [PubMed: 15564287]

Bagnyukova TV, Powell CL, Pavliv O, Tryndyak VP, Pogribny IP. Induction of oxidative stress and DNA damage in rat brain by a folate/methyl-deficient diet. Brain Res. 2008; 1237:44–51. [PubMed: 18694737]

Beaudin AE, Stover PJ. Insights into metabolic mechanisms underlying folate-responsive neural tube defects: a minireview. Birth Defects Res A Clin Mol Teratol. 2009; 85:274–84. [PubMed: 19180567]

Boyles AL, Wilcox AJ, Taylor JA, Shi M, Weinberg CR, Meyer K, Fredriksen A, Ueland PM, Johansen AM, Drevon CA, Jugessur A, Trung TN, Gjessing HK, Vollset SE, Murray JC, Christensen K, Lie RT. Oral facial clefts and gene polymorphisms in metabolism of folate/one-carbon and vitamin A: a pathway-wide association study. Genet Epidemiol. 2009; 33(3):247–255. [PubMed: 19048631]

Brooklyin S, Jana R, Aravinthan S, Adhisivam B, Chand P. Assessment of folic Acid and DNA damage in cleft lip and cleft palate. Clin Pract. 2014; 4:608. [PubMed: 24847430]

Burgoon JM, Selhub J, Nadeau M, Sadler TW. Investigation of the effects of folate deficiency on embryonic development through the establishment of a folate deficient mouse model. Teratology. 2002; 65:219–27. [PubMed: 11967921]

Chang H, Zhang T, Zhang Z, Bao R, Fu C, Wang Z, Bao Y, Li Y, Wu L, Zheng X, Wu J. Tissue-specific distribution of aberrant DNA methylation associated with maternal low-folate status in human neural tube defects. J Nutr Biochem. 2011; 22:1172–7. [PubMed: 21333513]

Choi SW, Friso S, Keyes MK, Mason JB. Folate supplementation increases genomic DNA methylation in the liver of elder rats. Br J Nutr. 2005; 93:31–5. [PubMed: 15705222]

Crott JW, Liu Z, Keyes MK, Choi SW, Jang H, Moyer MP, Mason JB. Moderate folate depletion modulates the expression of selected genes involved in cell cycle, intracellular signaling and folate uptake in human colonic epithelial cell lines. J Nutr Biochem. 2008; 19:328–35. [PubMed: 17681772]

de Croze N, Maczkowiak F, Monsoro-Burq AH. Reiterative AP2a activity controls sequential steps in the neural crest gene regulatory network. Proc Natl Acad Sci U S A. 2011; 108:155–60. [PubMed: 21169220]

Dhawan, A.; Bajpayee, M.; Pandey, AK.; P, D. Protocol for the single cell gel electrophoresis/comet assay for rapid genotoxicity assessment. Indian Institute of Toxicology Research; India: 2009.

Dickinson AJ, Sive H. Development of the primary mouth in Xenopus laevis. Dev Biol. 2006; 295:700–13. [PubMed: 16678148]

Dickinson AJ, Sive HL. The Wnt antagonists Frzb-1 and Crescent locally regulate basement membrane dissolution in the developing primary mouth. Development. 2009; 136:1071–81. [PubMed: 19224982]

Elmore S. Apoptosis: a review of programmed cell death. Toxicol Pathol. 2007; 35:495–516. [PubMed: 17562483]

Finnell RH, Greer KA, Barber RC, Piedrahita JA. Neural tube and craniofacial defects with special emphasis on folate pathway genes. Crit Rev Oral Biol Med. 1998; 9:38–53. [PubMed: 9488247]

Finnell RH, Shaw GM, Lammer EJ, Brandl KL, Carmichael SL, Rosenquist TH. Gene-nutrient interactions: importance of folates and retinoids during early embryogenesis. Toxicol Appl Pharmacol. 2004; 198:75–85. [PubMed: 15236946]

George TC, Basiji DA, Hall BE, Lynch DH, Ortyn WE, Perry DJ, Seo MJ, Zimmerman CA, Morrissey PJ. Distinguishing modes of cell death using the ImageStream multispectral imaging flow cytometer. Cytometry A. 2004; 59:237–45. [PubMed: 15170603]

Greenberg JA, Bell SJ, Guan Y, Yu YH. Folic Acid supplementation and pregnancy: more than just neural tube defect prevention. Rev Obstet Gynecol. 2011; 4:52–9. [PubMed: 22102928]

Grenier J, Teillet MA, Grifone R, Kelly RG, Duprez D. Relationship between neural crest cells and cranial mesoderm during head muscle development. PLoS One. 2009; 4:e4381. [PubMed: 19198652]

Gu L, Wu J, Qiu L, Jennings CD, Li GM. Involvement of DNA mismatch repair in folate deficiency-induced apoptosis small star, filled. J Nutr Biochem. 2002; 13:355–363. [PubMed: 12088801]

Hans F, Dimitrov S. Histone H3 phosphorylation and cell division. Oncogene. 2001; 20:3021–7. [PubMed: 11420717]

Ho PI, Ashline D, Dhitavat S, Ortiz D, Collins SC, Shea TB, Rogers E. Folate deprivation induces neurodegeneration: roles of oxidative stress and increased homocysteine. Neurobiol Dis. 2003; 14:32–42. [PubMed: 13678664]

Ichi S, Costa FF, Bischof JM, Nakazaki H, Shen YW, Boshnjaku V, Sharma S, Mania-Farnell B, McLone DG, Tomita T, Soares MB, Mayanil CS. Folic acid remodels chromatin on Hes1 and Neurog2 promoters during caudal neural tube development. J Biol Chem. 2010; 285:36922–32. [PubMed: 20833714]

Jacox L, Sindelka R, Chen J, Rothman A, Dickinson A, Sive H. The extreme anterior domain is an essential craniofacial organizer acting through Kinin-Kallikrein signaling. Cell Rep. 2014a; 8:596–609. [PubMed: 25043181]

Jacox LA, Dickinson AJ, Sive H. Facial transplants in Xenopus laevis embryos. J Vis Exp. 2014b

Kao TT, Chu CY, Lee GH, Hsiao TH, Cheng NW, Chang NS, Chen BH, Fu TF. Folate deficiency-induced oxidative stress contributes to neuropathy in young and aged zebrafish–implication in neural tube defects and Alzheimer's diseases. Neurobiol Dis. 2014; 71:234–44. [PubMed: 25131448]

Kennedy AE, Dickinson AJ. Median facial clefts in Xenopus laevis: roles of retinoic acid signaling and homeobox genes. Dev Biol. 2012; 365:229–40. [PubMed: 22405964]

Kennedy AE, Dickinson AJ. Quantification of orofacial phenotypes in Xenopus. J Vis Exp. 2014a:e52062. [PubMed: 25407252]

Kennedy AE, Dickinson AJ. Quantitative analysis of orofacial development and median clefts in Xenopus laevis. Anat Rec (Hoboken). 2014b; 297:834–55. [PubMed: 24443252]

Lee MS, Bonner JR, Bernard DJ, Sanchez EL, Sause ET, Prentice RR, Burgess SM, Brody LC. Disruption of the folate pathway in zebrafish causes developmental defects. BMC Dev Biol. 2012; 12:12. [PubMed: 22480165]

Li GM, Presnell SR, Gu L. Folate deficiency, mismatch repair-dependent apoptosis, and human disease. J Nutr Biochem. 2003; 14:568–75. [PubMed: 14559107]

Li J, Shi Y, Sun J, Zhang Y, Mao B. Xenopus reduced folate carrier regulates neural crest development epigenetically. PLoS One. 2011; 6:e27198. [PubMed: 22096536]

Lucock M. Folic acid: nutritional biochemistry, molecular biology, and role in disease processes. Mol Genet Metab. 2000; 71:121–38. [PubMed: 11001804]

Martin SA, McCarthy A, Barber LJ, Burgess DJ, Parry S, Lord CJ, Ashworth A. Methotrexate induces oxidative DNA damage and is selectively lethal to tumour cells with defects in the DNA mismatch repair gene MSH2. EMBO Mol Med. 2009; 1:323–37. [PubMed: 20049736]

Marean A, Graf A, Zhang Y, Niswander L. Folic acid supplementation can adversely affect murine neural tube closure and embryonic survival. Hum Mol Genet. 2011; 20:3678–3683. [PubMed: 21693562]

Martinelli M, Girardi A, Cura F, Carinci F, Morselli PG, Scapoli L. Evidence of the involvement of the DHFR gene in nonsyndromic cleft lip with or without cleft palate. Eur J Med Genet. 2014; 57:1–4. [PubMed: 24361572]

Molloy AM, Kirke PN, Brody LC, Scott JM, Mills JL. Effects of folate and vitamin B12 deficiencies during pregnancy on fetal, infant, and child development. Food Nutr Bull. 2008; 29:S101–11. discussion S112–5. [PubMed: 18709885]

Momb J, Lewandowski JP, Bryant JD, Fitch R, Surman DR, Vokes SA, Appling DR. Deletion of Mthfd1l causes embryonic lethality and neural tube and craniofacial defects in mice. Proc Natl Acad Sci U S A. 2013; 110:549–54. [PubMed: 23267094]

Nieuwkoop, PD.; Faber, J. Normal Table of Xenopus Laevis (Daudin). Garland Publishing Inc; New York: 1967.

Noden DM, Francis-West P. The differentiation and morphogenesis of craniofacial muscles. Dev Dyn. 2006; 235:1194–218. [PubMed: 16502415]

Novakovic P, Stempak JM, Sohn KJ, Kim YI. Effects of folate deficiency on gene expression in the apoptosis and cancer pathways in colon cancer cells. Carcinogenesis. 2006; 27:916–24. [PubMed: 16361273]

O'Sullivan RJ, Kubicek S, Schreiber SL, Karlseder J. Reduced histone biosynthesis and chromatin changes arising from a damage signal at telomeres. Nat Struct Mol Biol. 2010; 17:1218–25. [PubMed: 20890289]

Porter AG, Janicke RU. Emerging roles of caspase-3 in apoptosis. Cell Death Differ. 1999; 6:99–104. [PubMed: 10200555]

Qi H, Ratnam M. Synergistic induction of folate receptor beta by all-trans retinoic acid and histone deacetylase inhibitors in acute myelogenous leukemia cells: mechanism and utility in enhancing selective growth inhibition by antifolates. Cancer Res. 2006 Jun 1; 66(11):5875–82. [PubMed: 16740727]

Rajagopalan PT, Zhang Z, McCourt L, Dwyer M, Benkovic SJ, Hammes GG. Interaction of dihydrofolate reductase with methotrexate: ensemble and single-molecule kinetics. Proc Natl Acad Sci U S A. 2002; 99:13481–6. [PubMed: 12359872]

Rogers EJ, Chen S, Chan A. Folate deficiency and plasma homocysteine during increased oxidative stress. N Engl J Med. 2007; 357:421–2. [PubMed: 17652662]

Schmidt J, Piekarski N, Olsson L. Cranial muscles in amphibians: development, novelties and the role of cranial neural crest cells. J Anat. 2013; 222:134–46. [PubMed: 22780231]

Shookhoff JM, Gallicano GI. A new perspective on neural tube defects: folic acid and microRNA misexpression. Genesis. 2010; 48:282–94. [PubMed: 20229516]

Simoes-Costa M, Bronner ME. Establishing neural crest identity: a gene regulatory recipe. Development. 2015; 142:242–257. [PubMed: 25564621]

Sive, HL.; Grainger, R.; Harlard, R. Early development of Xenopus laevis: a laboratory manual. Cold Spring Harbor Laboratory Press; 2000.

Soto M, Iborra S, Quijada L, Folgueira C, Alonso C, Requena JM. Cell-cycle-dependent translation of histone mRNAs is the key control point for regulation of histone biosynthesis in Leishmania infantum. Biochem J. 2004; 379:617–25. [PubMed: 14766017]

Sun J, Sugiyama A, Inoue S, Takeuchi T, Furukawa S. Effect of methotrexate on neuroepithelium in the rat fetal brain. J Vet Med Sci. 2014; 76:347–54. [PubMed: 24200895]

Sun S, Gui Y, Jiang Q, Song H. Dihydrofolate reductase is required for the development of heart and outflow tract in zebrafish. Acta Biochim Biophys Sin (Shanghai). 2011; 43:957–69. [PubMed: 22113051]

Sun SN, Gui YH, Wang YX, Qian LX, Jiang Q, Liu D, Song HY. Effect of dihydrofolate reductase gene knock-down on the expression of heart and neural crest derivatives expressed transcript 2 in zebrafish cardiac development. Chin Med J (Engl). 2007; 120:1166–71. [PubMed: 17637246]

Szabo-Rogers HL, Smithers LE, Yakob W, Liu KJ. New directions in craniofacial morphogenesis. Dev Biol. 2010; 341:84–94. [PubMed: 19941846]

Tang LS, Santillano DR, Wlodarczyk BJ, Miranda RC, Finnell RH. Role of Folbp1 in the regional regulation of apoptosis and cell proliferation in the developing neural tube and craniofacies. Am J Med Genet C Semin Med Genet. 2005; 135C:48–58. [PubMed: 15800851]

Taylor W, VD G. Revised procedures for staining and clearing small fishes and other vertebrates for bone and cartilage study. Cybium. 1985; 9:107–119.

Wang X, Wang J, Guan T, Xiang Q, Wang M, Guan Z, Li G, Zhu Z, Xie Q, Zhang T, Niu B. Role of methotrexate exposure in apoptosis and proliferation during early neurulation. J Appl Toxicol. 2014; 34:862–9. [PubMed: 23836430]

Wehby GL, Murray JC. Folic acid and orofacial clefts: a review of the evidence. Oral Dis. 2010; 16:11–9. [PubMed: 20331806]

Wheeler GN, Brandli AW. Simple vertebrate models for chemical genetics and drug discovery screens: lessons from zebrafish and Xenopus. Dev Dyn. 2009; 238:1287–308. [PubMed: 19441060]

Wilcox AJ, Lie RT, Solvoll K, Taylor J, McConnaughey DR, Abyholm F, Vindenes H, Vollset SE, Drevon CA. Folic acid supplements and risk of facial clefts: national population based case-control study. BMJ. 2007; 334:464. [PubMed: 17259187]

Winning RS, Shea LJ, Marcus SJ, Sargent TD. Developmental regulation of transcription factor AP-2 during Xenopus laevis embryogenesis. Nucleic Acids Res. 1991; 19:3709–14. [PubMed: 1852613]

Wu D, Ingram A, Lahti JH, Mazza B, Grenet J, Kapoor A, Liu L, Kidd VJ, Tang D. Apoptotic release of histones from nucleosomes. J Biol Chem. 2002; 277:12001–8. [PubMed: 11812781]

Zhang XM, Huang GW, Tian ZH, Ren DL, W JX. Folate deficiency induces neural stem cell apoptosis by increasing homocysteine in vitro. J Clin Biochem Nutr. 2009; 45:14–9. [PubMed: 19590702]

Zhao J, Guan T, Wang J, Xiang Q, Wang M, Wang X, Guan Z, Xie Q, Niu B, Zhang T. Influence of the antifolate drug Methotrexate on the development of murine neural tube defects and genomic instability. J Appl Toxicol. 2013; 33:915–23. [PubMed: 22806879]

Zhao R, Goldman ID. Resistance to antifolates. Oncogene. 2003; 22:7431–57. [PubMed: 14576850]

Highlights

- DHFR is required in the face during early orofacial development
- Apoptosis is a major contributor of DHFR inhibition induced facial abnormalities.
- A reduction in cell proliferation is a minor contributor to DHFR inhibition induced facial abnormalities
- Abrogated folate metabolism can reduce or exacerbate retinoic acid inhibition induced orofacial clefts.
- Folinic acid supplementation increases cell survival in embryos treated with a RAR inhibitor.

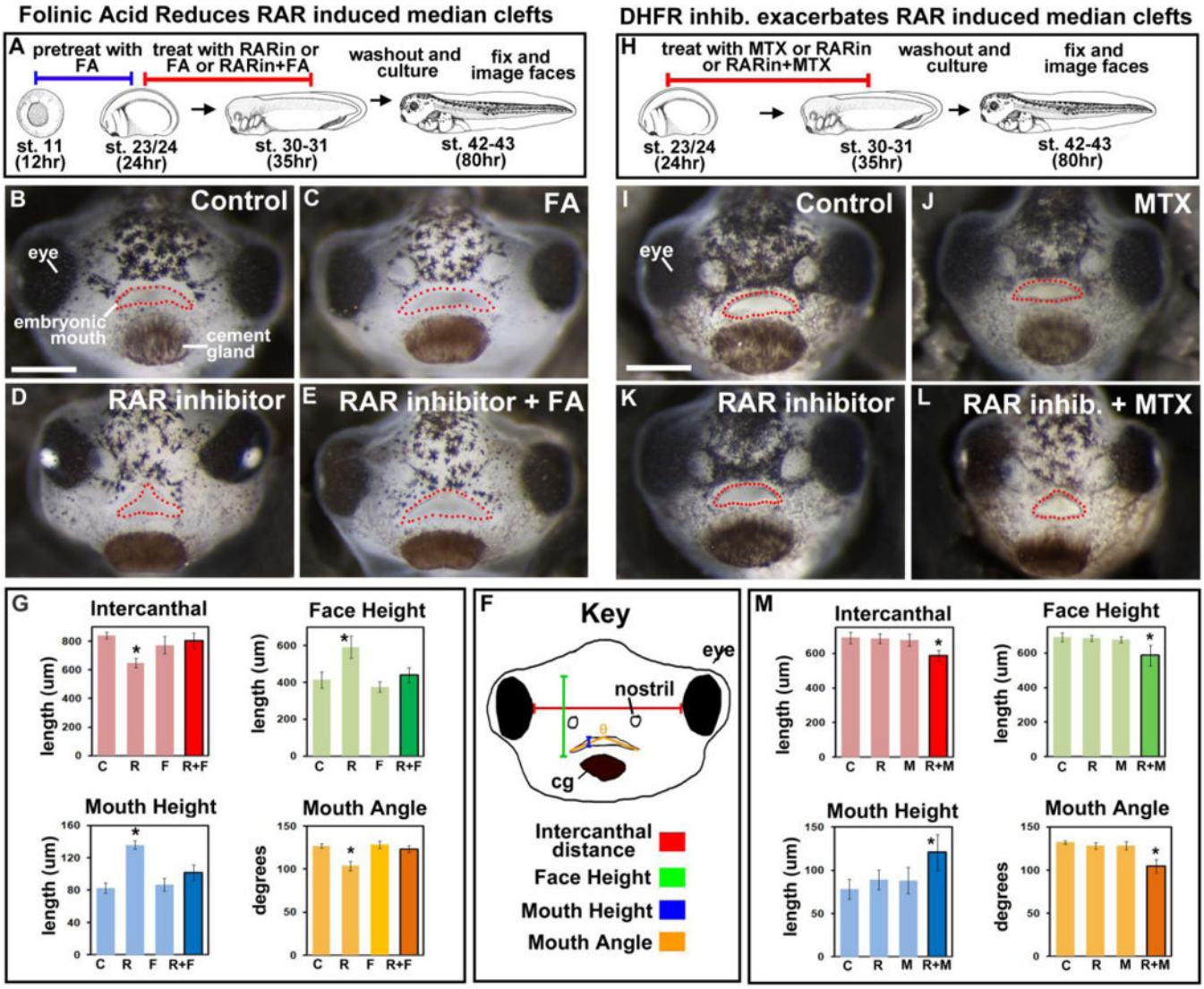

Figure 1.

Folate and retinoic acid signaling. A) Schematic of the experimental design for B–G (2 experiments and n=20). B–C) Representative frontal views of faces at stage 42–43 treated with DMSO (B) or folinic acid (C) RAR inhibitor (D), or RAR inhibitor and folinic acid (E). F) Schematic of the facial dimensions measured. G) Bar graphs summarizing quantification of facial dimensions corresponding to B–E. H) Schematic of experimental design for I–M (2 experiments, n=20). I–L). Representative frontal views of faces at stage 42 treated with DMSO (I) or MTX (J) RAR inhibitor (K), or RAR inhibitor and MTX (L). M) Bar graphs summarizing quantification of facial dimensions corresponding to I–L. Mouth is outlined with red dots in all frontal views and asterisks designate statistical significance with all p values < 0.001. All images are at the same magnification, scale bar =175 μm. Abbreviations: C=control, R=RAR inhibitor, F=folinic acid, M=methotrexate.

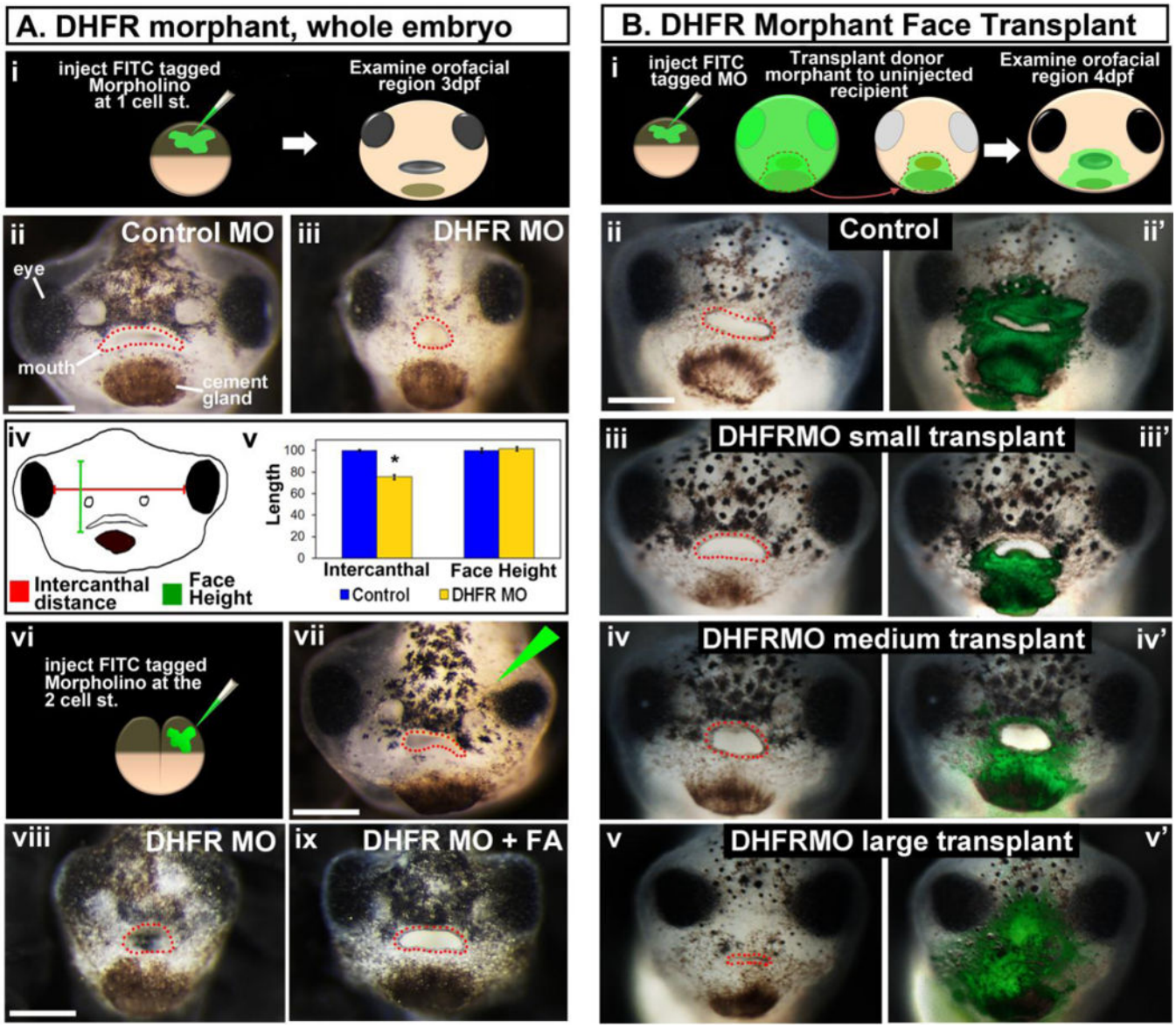

Figure 2.

DHFR morpholino knockdown results in abnormal orofacial development. A) Whole DHFR morphant analysis. i) Schematic showing the experimental design. ii,iii) Representative frontal views of faces injected with control (ii) or DHFR (iii) morpholinos. iv) Schematic of facial dimensions measured. v) Bar graph showing quantification of facial dimensions normalized to the controls (set to 100), asterisk designates statistical significance for 2 experiments (n=60) p value < 0.001. vi) Schematic showing the experimental design for vii. vii) Representative frontal view of the face of an embryo injected in one cell as shown in vi. The injected side is indicated by the green triangle. viii, ix) rescue experiment showing representative frontal views of faces injected with DHFR MO (viii) or DHFR MO and treated with folinic acid (FA) (ix). B) Localized DHFR morpholinos using face transplants. i) Schematic of the experimental design. ii–v') Representative frontal views of embryos that received DHFR morphant tissue. Prime roman numerals are composites of the unprimed

counterpart with fluorescent overlays showing the location of morpholino containing tissue (n= 2 experiments, n=11). All embryos were imaged at same magnification, scale bar = 200 μm. The mouth is outlined in red dots.

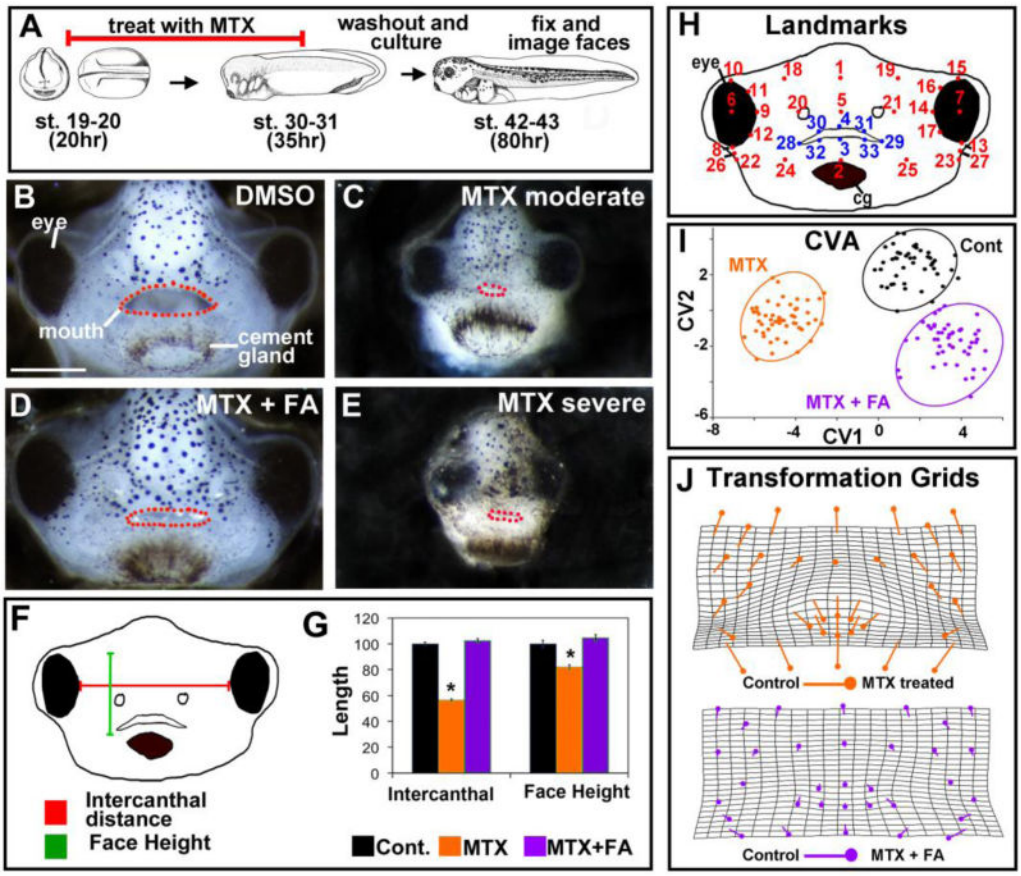

Figure 3.

Pharmacological inhibition of DHFR alters size and shape of the face. A) Schematic of the experimental design. B–E) Representative frontal views of faces treated with DMSO (B), 220 μM MTX (C, E) and 220 μM MTX + folinic acid (FA) (D). All images were taken at same magnification (scale bar =150μm). Mouth is outlined in red dots. F) Schematic of the facial dimensions measured. G) Bar graphs of the quantification of facial dimensions for 2 experiments (n=20). Asterisks designate statistical difference when compared to control (all p values ≤ 0.001). H) Landmark locations for morphometric analysis. I) Canonical variate analysis of landmark coordinates. Statistically significant for 2 experiments, n=10, p value ≤0.05). J) Transformation grids showing the change in landmark position in MTX treated embryos compared to controls (top grid) and controls compared to rescued embryos (bottom grid).

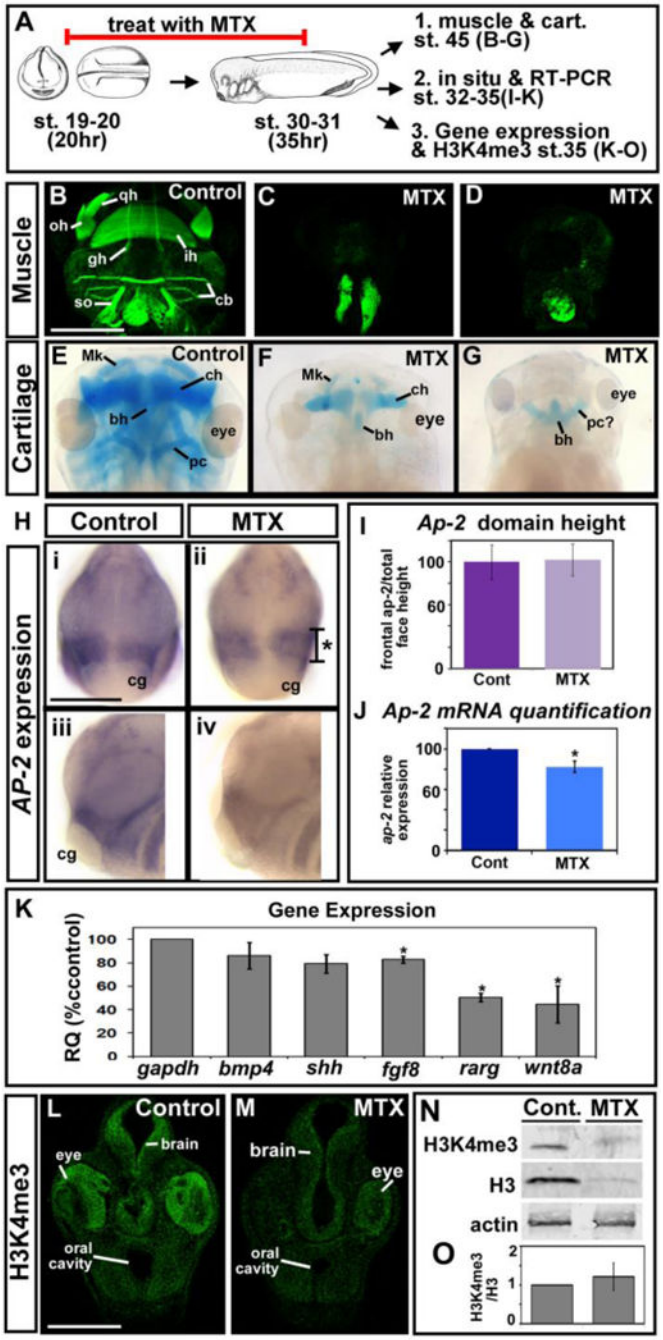

Figure 4.

Inhibition of DHFR alters jaw muscle and cartilage, gene expression and total histone levels. A) Schematic of the experimental design. B–D) Representative ventral views of embryos labeled with phalloidin to mark muscle. Images are all at the same magnification (scale bar =500 μm), 2 experiments (n=14). E–G) Representative dorsal views of embryos labeled with Alcian blue to show cartilage. Images are all at the same magnification (scale bar =500 μm), 2 experiments (n=20). H) in-situ hybridization for neural crest marker, AP-2, frontal views (i, ii) and lateral views with anterior to the left (iii, iv). All images are at the same

magnification (scale bar = 175 μm). Asterisk designates the region measured and graphed in I. I) Bar graph showing quantification of the AP-2 domain in the face. There is no statistical significance in 2 experiments (n=12, p value = 0.64). J) Bar graph showing quantification of AP-2 mRNA levels by qRT-PCR. Statistical significance designated by asterisk, 2 experiments. K) mRNA levels of genes expressed in the face relative to GAPDH. Asterisks designate statistical significance (p values for significance are all ≤ 0.005). M–N) Immunohistochemistry of H3K4me3 in representative transverse sections of the face (2 experiments, n=10). Images are at the same magnification (scale bar =100 μm). N) Representative western blot of H3K4me3, total H3 and actin (n=2 experiments). P) The ratio of H3k4me3 to H3 from 2 experiments is not statistically different (p value=0.589). Abbreviations; gh=Geniohyoideus, ih=Interhyoideus, so=Subarcualis obliquus II, oh=Orbitohyoideus, qh=Quadrato-hyo-angularis, cb=Constrictores branchialium, Mk= Meckel's cartilage, ch= ceraohyal cartilage, bh=basihyal cartilage, pc=parachordal cartilage.

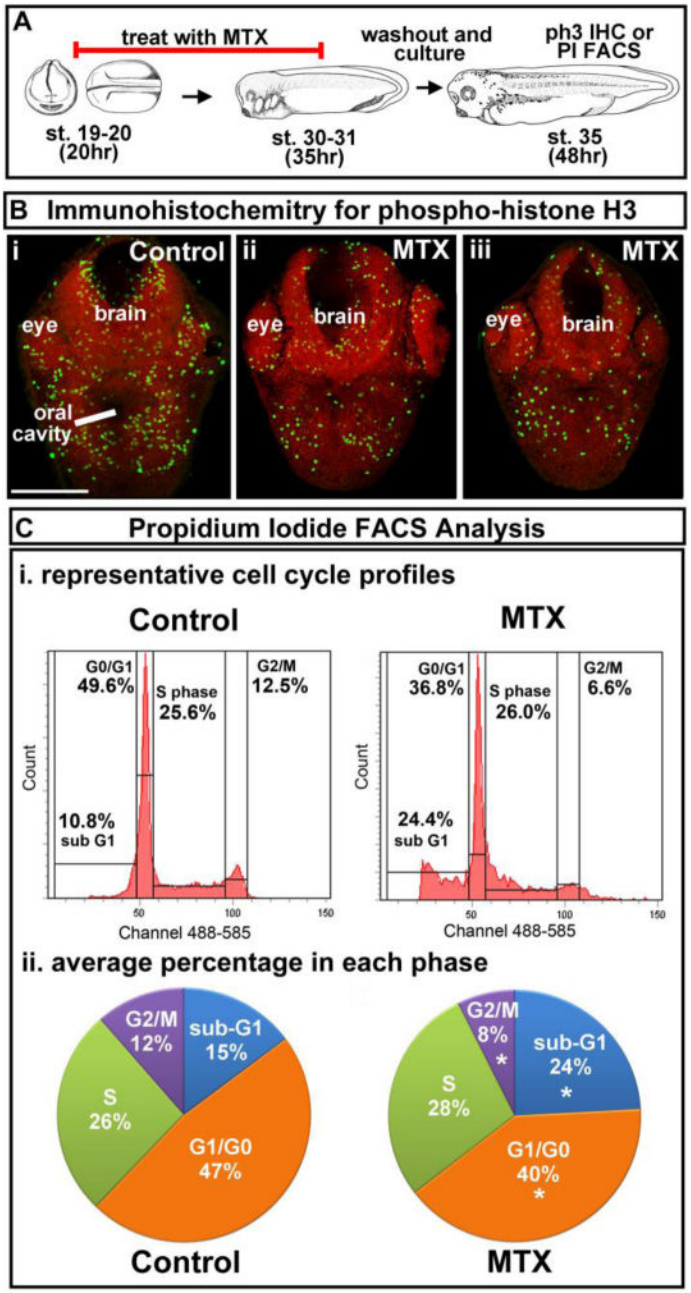

Figure 5.

Cell proliferation is decreased in MTX treated embryos. A) Schematic of the experimental design. B) Immunohistochemistry of pH3 in representative transverse sections of the face from embryos treated with DMSO (i), or MTX (ii,iii). Images are all at the same magnification, scale bar =100 μm. C) FACS analysis of the cell cycle. i) Representative cell cycle profiles. ii) The average percentages of cells in each fraction from 4 experiments. Statistical significance was determined using Mann Whitney U test and designated by asterisks (p values ≤ 0.028).

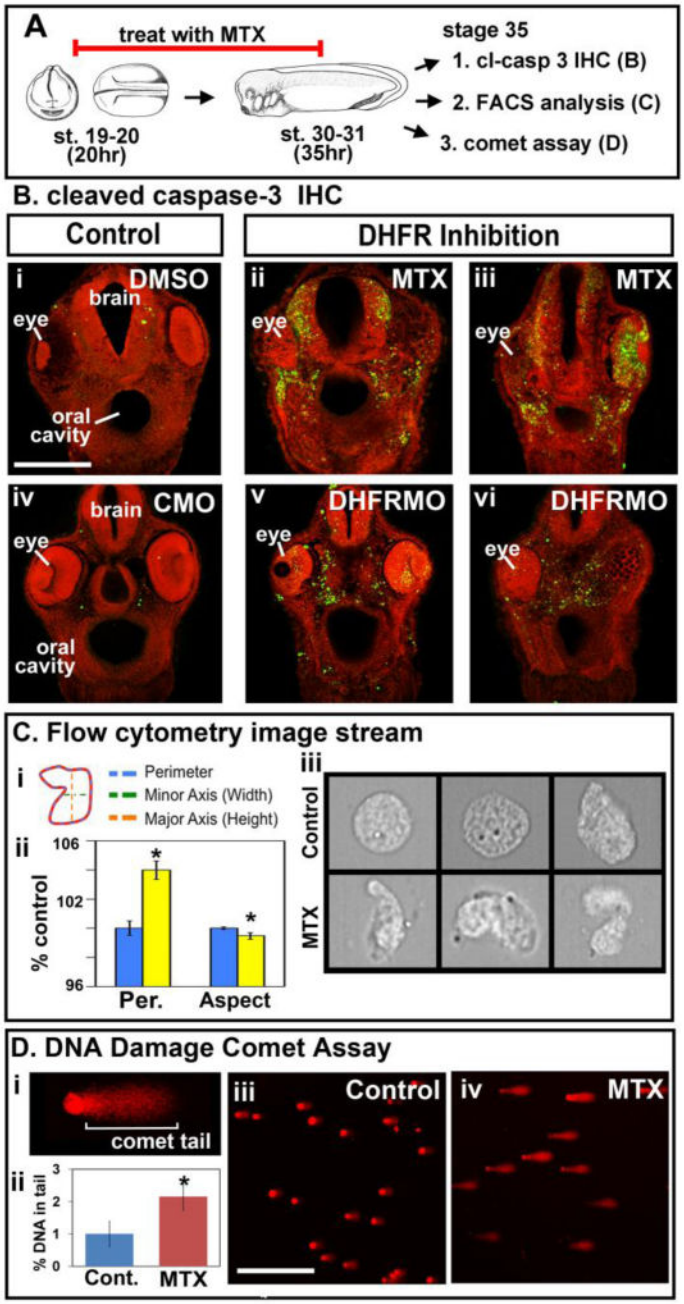

Figure 6.

DHFR inhibition results in increased apoptosis and DNA damage. A) Schematic of the experimental design. B) Immunohistochemistry of cleaved caspase-3 (green) in transverse sections of the face from embryos treated with DMSO (i), or MTX (ii,iii) or injected with control morpholino (CMO)(iv) or DHFR morpholinos (DHFRMO) (v,vi). Images are all at the same magnification (scale bar =100 μm) and counterstained with propidium iodide. C) Imagestream flow cytometry to analyze cell morphology. Ci) Schematic showing cellular measurements used in the analysis. Cii) Bar graph showing average perimeter (Per.) and Aspect ratio (Aspect) (major/minor axis). Statistical significance designated by asterisks (p

values ≤ 0.05). Ciii) Representative images of single cells acquired by the ImageStream. D) Comet assay for DNA damage. Di) Representative cell to show the comet tail region where fluorescence was quantified. Dii) Bar graph showing quantification of fluorescence in comet tails from cells isolated in two experiments. Statistical significance is designated by an asterisk (n=40 cells, p value = 6.8E–06). Diii,iv) Representative images of cells from comet assay. Scale bar= 50μm.

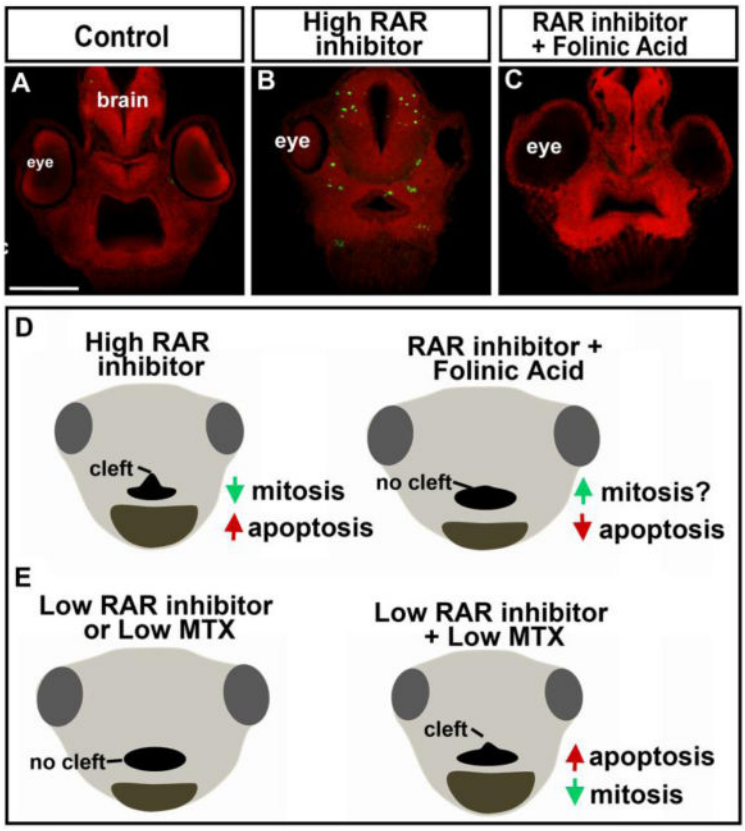

Figure 7.

Mechanism of folate and retinoic acid signaling interaction. A–B) Representative transverse sections through the face labeled with cleaved caspase-3 (green) and counterstained with propidium iodide. This was consistent in at least 10 embryos at equivalent locations in the face All images were taken at the same magnification, scale bar=175μm. D) Model of how folinic acid supplementation prevents median orofacial clefts. E) Model of the mechanism by which RAR and DHFR inhibition could synergize.